International Immunopharmacology 117 (2023) 109951

Contents lists available at ScienceDirect

International Immunopharmacology

journal homepage: www.elsevier.com/locate/intimp

Thymosin beta 4 prevents systemic lipopolysaccharide-induced plaque load in middle-age APP/PS1 mice

Othman Othman [a], Hayley Marshall [a], Mitchell Masterson [a], Poppy Winlow [a], Graham Gibson [b], Yuchun Ding [c], Marie-Christine Pardon [a,*]

[a] School of Life Sciences, Division of Physiology, Pharmacology & Neuroscience, University of Nottingham Medical School, Queens Medical Centre, Nottingham NG7 2UH, United Kingdom
[b] Nottingham University Hospitals NHS Trust, Department of Histopathology, Queens Medical Centre, Nottingham NG7 2UH, United Kingdom
[c] School of Computer Sciences, University of Nottingham, Jubilee Campus, Wollaton Road, Nottingham NG8 1BB, United Kingdom

ARTICLE INFO

Keywords:
Lipopolysaccharide
Thymosin beta 4
Alzheimer's disease
Amyloid load
Gliosis
LPS-induced sickness

ABSTRACT

Lipopolysaccharide (LPS) produced by the gut during systemic infections and inflammation is thought to contribute to Alzheimer's disease (AD) progression. Since thymosin beta 4 (Tβ4) effectively reduces LPS-induced inflammation in sepsis, we tested its potential to alleviate the impact of LPS in the brain of the APPswePS1dE9 mouse model of AD (APP/PS1) and wildtype (WT) mice. 12.5-month-old male APP/PS1 mice (n = 30) and their WT littermates (n = 29) were tested for baseline food burrowing performance, spatial working memory and exploratory drive in the spontaneous alternation and open-field tests, prior to being challenged with LPS (100ug/kg, i.v.) or its vehicle phosphate buffered saline (PBS). Tβ4 (5 mg/kg, i.v.) or PBS, was administered immediately following and at 2 and 4 h after the PBS or LPS challenge, and then once daily for 6 days (n = 7–8). LPS-induced sickness was assessed though monitoring of changes in body weight and behaviour over a 7-day period. Brains were collected for the determination of amyloid plaque load and reactive gliosis in the hippocampus and cortex. Treatment with Tβ4 alleviated sickness symptoms to a greater extent in APP/PS1 than in WT mice by limiting LPS-induced weight loss and inhibition of food burrowing behaviour. It prevented LPS-induced amyloid burden in APP/PS1 mice but increased astrocytic and microglial proliferation in the hippocampus of LPS-treated WT mice. These data show that Tβ4 can alleviate the adverse effects of systemic LPS in the brain by preventing exacerbation of amyloid deposition in AD mice and by inducing reactive microgliosis in aging WT mice.

1. Introduction

Systemic infection and inflammation are well established risk factors for the progression of Alzheimer's disease (AD) [1,2], the major senile dementia characterised by a progressive cognitive decline associated with brain atrophy and the accumulation of toxic beta-amyloid (Aß) plaques and neurofibrillary tangles made of hyperphosphorylated tau. Infectious events can also contribute to inflammaging, a state of low-grade chronic systemic inflammation associated with dysfunctional immunity and a risk factor for AD, which frequently occurs with ageing in the absence of overt infection, potentially leading to increased susceptibility to infections and up-regulation of certain pro-inflammatory markers in blood and tissues [3,4].

In this context, the endotoxin hypothesis of neurodegeneration stipulates that excess levels of lipopolysaccharide (LPS), a gram-negative bacteria produced by the gut during systemic inflammation and infections, plays a key role in promoting Aß and tau aggregation [5]. While LPS would not normally cross the blood brain barrier due to its large size, it has been found in the brain of AD patients and to co-localise with Aß plaques [6]. Circulating levels of LPS are also increased in the blood of AD patients [7], which is favoured by an increased permeability of the epithelial gut barrier, promoting entry of LPS to the brain due to an associated blood-brain barrier dysfunction [8]. Studies in rodent models of AD have also established that LPS either endogenous or exogenously administered can penetrate the brain and accelerate the progression of key hallmarks AD, suggesting that strategies to control LPS -induced inflammation have the potential to halt AD progression [9].

LPS is also recognized as the most potent microbial mediator implicated in the pathogenesis of sepsis and septic shock, a life-

* Corresponding author.
E-mail address: marie.pardon@nottingham.ac.uk (M.-C. Pardon).

https://doi.org/10.1016/j.intimp.2023.109951
Received 28 November 2022; Received in revised form 16 February 2023; Accepted 20 February 2023
Available online 4 March 2023

threatening systemic inflammatory syndrome [10]. Thymosin beta 4 (Tß4) is a ubiquitously expressed peptide [11] with potent anti-inflammatory properties which has been found highly effective in reducing sepsis-like symptoms in human and animals [12,13]. Circulating levels of Tß4 are reduced in sepsis [12,13] and supplementation with Tß4 immediately following LPS administration in rodents was shown to increase survival and limit the production of pro-inflammatory cytokines [13]. Using a low-dose LPS more relevant to low-grade inflammation than sepsis, and which effectively elevates circulating levels of pro-inflammatory cytokines and sickness symptoms [14,15], we tested the potential of Tβ4 to alleviate the impact of systemic LPS-induced sickness, Aß plaque load and associated gliosis in a transgenic mouse model of amyloidosis.

2. Materials and methods

2.1. Ethics statement

All procedures were carried out in accordance with the UK Animals (Scientific Procedures) Act of 1986 under project license 40/3601, approved by the University of Nottingham Ethical Review Committee and are reported according to the ARRIVE guidelines [16]. All analyses were performed in blind.

2.2. Animals and husbandry

Sixty 12.5-month-old experimentally naïve APPswe/PS1dE9 (APP/PS1 [17]) male mice (n = 30), and their wild-type (WT) littermates (n = 30), were initially used but one WT mouse was excluded as it combined obesity with behavioural abnormalities and signs of systemic illness in the abdomen. All experimental animals were bred in the university of Nottingham Biomedical Service Unit from a breeding stock of APPswe/PS1dE9 mice, originally purchased from the Jackson Laboratories (stock # 34832-JAX). Mice were initially maintained grouped housed (n = 3–4 per cage) in individually ventilated cages under standard husbandry conditions with ad libitum access to food and water as well as access to a play tube and nesting material. They were then singly housed in the same standard husbandry conditions one week prior to the start of the experiment, as this was required for food burrowing behaviour. The rooms were on a 12 h light/dark cycle with lights on at 07:00; temperature, humidity and air exchange were automatically controlled.

2.3. Drug treatments

Lipopolysaccharide (LPS, Escherichia coli serotype 0111:B4, Sigma Aldrich, UK) and thymosin beta 4 (Tß4, a generous gift from RegeneRx Biopharmaceuticals, Rockville, MD, USA) were prepared as stock solutions in sterile phosphate buffered saline (PBS, Sigma Aldrich) and stored in aliquots at −20 °C until use. On the day of the experiment, LPS and Tß4 were further diluted 1:2 in PBS to final concentrations of 100 μg/ml and 2.5 mg/ml, respectively. Mice were injected intravenously (i.v.) in the lateral tail vein with 100 μg/kg of LPS [14,18] and/or 5 mg/kg of Tß4 [13] and/or an equivalent volume (1 μl/g of body weight) of their vehicle PBS.

2.4. Study design

The timeline of the experiment is depicted Fig. 1A. 12.5-month-old APP/PS1 and WT mice were randomly allocated to the four treatment groups: PBS, Tß4, LPS or LPS+Tß4 (n = 7–8/group). Baseline behavioural assessment was carried out on the 3 days preceding the LPS injection. Mice underwent baseline food burrowing testing in their home cage for 3 days. They were also tested for baseline spatial working memory performance and exploratory drive in the spontaneous alternation test (Day −1) and baseline locomotor performance in the open field test (Day 0) prior to the start of the treatments. Tß4 (5 mg/kg i.v.) or PBS (2 μl/g of body weight) was administered immediately following, and at 2 and 4 h after a low LPS dose (100 μg/kg i.v.) or PBS (1 μl/g of body weight), as this was proven to be the most effective treatment regimen against septic doses of LPS [13], and then once daily for the next 6 days. To monitor the recovery from LPS-induced sickness behaviour, locomotor suppression in the open-field was recorded at 2, 4, 6 and 24 h post LPS, and again on Days 3 and 7, together with spontaneous alternation behaviour. Body weight and food burrowing performance were recorded daily for the 7 days post LPS. On Day 7, immediately after the spontaneous alternation task, mice were culled by cervical dislocation and trunk blood was collected. Their brains were removed; the cortex and hippocampus were dissected from one hemisphere, snap frozen and stored at −80 °C until use. The second hemisphere was post-fixed by immersion in 4% paraformaldehyde, stored at 4–8 °C for a minimum of 24 h, and then embedded in paraffin wax on a tissue embedding station (Leica TP1020). One week was chosen as the duration of the experiment to both enable detecting changes in amyloid plaque load [19,20] and monitor the recovery of LPS-induced sickness, which is expected to take longer than 3 days in ageing mice [21].

2.5. Behavioural assessment

2.5.1. Food burrowing

Food burrowing is a species-specific behaviour largely dependent of the integrity of the hippocampus [22], which is suppressed in response to systemic administration of LPS [15]. The protocol was adapted from one previously described [14,15]. A glass jar containing 30 g of food pellets broken into small pieces was added to the home cage with ad libitum access to food and water. The amount of food displaced from the jar was recorded daily, expressed as a percentage from the 30 g provided, and used as a measure of food burrowing performance. The jar was refilled daily. The first baseline recording was used as an indication of baseline genotype differences, while data from the next two days were averaged and used a baseline level of performance for the monitoring of LPS-induced sickness.

2.5.2. Spontaneous alternation

Spontaneous alternation was used as previously described [14] to assess spatial working memory and exploratory drive. The Y-shaped maze comprised three identical transparent Plexiglas® arms at a 120° angle from each other (41.5 cm in length and 6 cm in width surrounded by 15 cm high transparent Perspex walls). The start point (6 cm × 7.5 cm) was in the centre of the maze, and the mice were allowed to freely explore the three arms over five minutes. The number of alternations was recorded manually and expressed as a percentage of alternations to estimate spatial working memory performance, while the number of arms visited was used as an indication of exploratory drive. To assess sickness effects, the difference between pre- and post-injection performance was calculated and expressed as a percentage of the baseline performance. One mouse had to be excluded from the analysis of the 7-day time point as it entered only one arm, and therefore its alternation rate could not be calculated.

2.5.3. Open field

Mice were placed into the open field arena (dark-grey plexiglass floor, surrounded by transparent plexiglass walls, 30 cm long × 35 cm wide × 30 cm high) for 3 mins prior to and at 2, 4, 6, 24 h and 72 h post LPS, and for 15 mins on day 7. The total distance covered by the mice in the whole arena was automatically tracked using the Ethovision software (v. XT7, Noldus, Wageningen, Netherlands) and used to monitor LPS-induced behavioural suppression.

2.6. Immunohistochemical analyses

2.6.1. Immunohistochemistry

7 μm-thick coronal sections were cut throughout the hippocampus

using a microtome (Microtome Slee Cut 4060), mounted on Surgipath X-tra Adhesive slides (Leica Biosystems, Milton Keynes, UK), and dried overnight at 40 °C. Immunostaining of the microglial marker Ionized calcium binding adaptor molecule 1 (Iba1), the astrocyte marker glial fibrillary acidic protein (GFAP) and amyloid plaques was carried out with an automated immunostainer (Ventana BenchMark ULTRA) in 6–8 brain slices per brain. Slices were incubated with the following primary antibodies: rabbit anti-Iba1 (Wako, cat. nr. 019–19741; 1:500) or anti-GFAP (Biogenix, cat. nr. AM020-5M, 1:5000) or anti-Aß (Agilent, cat. nr. M0872, 1:50). The primary antibodies were subsequently detected using the ultraView Universal DAB Detection Kit (Roche Diagnostics Ltd). Finally, the slides were counterstained with hematoxylin. Digital focused photo-scanning images were then acquired using a Hamamatsu NanoZoomer-XR 2.0-RS C10730 digital scanning system with TDI camera technology a NanoZoomer (Hamamatsu Photonics K.K. Systems, Japan) at 20× magnification and visualised using NDP.view2 (NanoZoomer Digital Photography).

2.6.2. Semi-automated quantification of Iba1, GFAP and amyloid staining

Segmentation of microglia, astrocytes and amyloid plaques, and extraction of morphometric features, was performed using custom made Matlab codes adapted from our previous studies [14,18,23], and applied to the whole hippocampus and whole cortex. This provided the percentage area occupied by glial cells and amyloid plaques, the number of Iba1- and GFAP-positive cells, used as a measure of microglial and astrocyte density, respectively, the size of microglial somas, used as a morphometric marker of microglia activation and known to be sensitive to LPS [18], the number of microglia clusters, the number and area of amyloid plaques, used as an indicator of amyloid plaque load, and, using established criteria [24], the number of small ($\leq$400 μm^2), medium (401 μm^2–700 μm^2) and large (>700 μm^2) plaques, used as an indicator of plaque development and maturation.

2.7. Elisas

Diethylamine (DEA) was used to extract non-plaque associated soluble $A\beta_{1\text{-}40}$ and amyloid precursor protein (APP) from cortical tissue using standard protocols [25]. Briefly, cortices were homogenised in tissue homogenisation buffer (2 mM Tris -pH7.4-, 250 mM sucrose, 0.5 mM EDTA, 0.5 mM EGTA) at a concentration of 100 mg tissue/mL on ice, then diluted 1:2 in 0.4% DEA solution in 100 mM NaCl and centrifuged at 135,000 g for 1 h at 4 °C. The supernatant, which contains the soluble fraction, was collected, neutralised with 1/10 vol of 0.5 M Tris HCl (pH 6.8), aliquoted and stored at −80 °C. Cortical levels of APP and $A\beta_{1\text{-}40}$ were assayed using commercially available Elisa's kits (Invitrogen, catalog #KHB0051 & KHB3481, respectively) according to the manufacturer's instructions with a dilution of 1:25 for APP and 1:50 for $A\beta_{1\text{-}40}$. Data was calculated as a ratio of protein content, determined using a BCA protein assay kit (Millipore, catalogue #71285).

2.8. Data analysis

Data are presented as mean ± SEM (standard error of the mean) or median ± interquartile range and were analysed using InVivoStat [26].

Genotype-related differences in baseline measures, taken prior to any drug administration, were analysed using unpaired *t*-tests or Mann Whitney test (food burrowing data). For the assessment of the progression of LPS-induced sickness, all data, but food burrowing data, were expressed as percent of baseline value to account for a possible confounding effect of baseline differences between treatment groups. The impact of LPS and/or Tβ4 on behavioural, physiological, and histological measures was analysed using two or three-way ANOVAs or ANCOVAs with LPS, Tβ4, and where applicable, genotype, as between subject-factors and, where applicable, repeated measures over time. Food burrowing data were expressed as % food burrowed, and rank transformed prior to repeated measure ANOVA, to normalise the distribution. For all other *in vivo* measures, baseline measurements were used as covariate. The number of microglial clusters was also used as a covariate for the analysis of microglia features, as described previously [18]. This was followed, when appropriate, by post-hoc planned comparisons. The following pairwise comparisons were decided a priori, for each time point: i) PBS-treated WT vs APP/PS1 mice to test for genotype differences; ii) PBS vs LPS for each genotype to test for the impact of LPS alone iii) PBS *vs* Tβ4 in each genotype, to test for the effect of Tβ4 on all measures in the absence of LPS, iv) PBS and LPS *vs* LPS+ Tβ4 in each genotype to test for the effectiveness of Tβ4 on LPS-induced changes and v) within each treatment group, each time point *vs* baseline to test for the progression of LPS-induced sickness.

3. Results

3.1. Tβ4 alleviates LPS-induced "sickness" in APP/PS1 mice

3.1.1. Tβ4 limits LPS-induced weight loss in APP/PS1 mice

WT and APP/PS1 mice did not differ for baseline body weight measurements taken on Day 0 prior to the LPS challenge ($t_{(55)} = -0.15$, $p = 0.878$; Fig. 1B). LPS caused a persistent reduction in body mass in both genotypes that was significantly greater than the weight loss caused by repeated measurements in the absence of LPS (LPS X Time: $F_{(7,357)} = 14.67$, $p < 0.0001$; Fig. 1C). Fluctuations in body weight with time were also dependent upon treatment with Tβ4 (LPS X Tβ4 X Time: $F_{(7,357)} = 3.01$, $p = 0.004$). A 7-day treatment with Tβ4 from the onset of LPS-induced systemic inflammation alleviated the resulting weight loss in both genotypes, but this was overall more pronounced in LPS-treated APP/PS1 mice ($p < 0.0001$ for APP/PS1 and $p = 0.38$ for WT mice) with significant benefits seen from the third day post LPS until the end of the experiment ($p < 0.05$ *vs* LPS at all time points, Fig. 1C).

3.1.2. Tβ4 improved food burrowing behaviour in APP/PS1 mice

WT and APP/PS1 mice did not significantly differ for baseline food burrowing behaviour over of the 3 days ($F_{(1,57)} = 3.11$, $p = 0.08$; Fig. 1D, E & F), but their performance improved with time ($F_{(2,114)} = 14.81$, $p < 0.0001$). The amount of food displaced was significantly lower on the first measurement regardless of the genotype ($p < 0.01$ *vs* 2nd and 3rd measurements for both WT and APP/PS1 mice) but did not differ significantly between the second and third day prior the start of the treatment ($p = 0.97$ and 0.29 for WT and APP/PS1 mice, respectively). The average of the second and third measurements was therefore used as pre-treatment baseline performance for the monitoring of LPS-induced sickness and Tβ4 treatment. Overall, the performance of APP/PS1 mice throughout the experiment was lower than seen in WT mice, regardless of the treatment condition ($F_{(1,51)} = 6.98$, $p = 0.01$; Fig. 1G&H). LPS suppressed food burrowing behaviour in both genotypes, regardless of treatment with Tβ4 ($F_{(1,51)} = 10.02$, $p = 0.003$; Fig. 1H), with performances significantly lower than baseline values for 3 days in all groups ($p \leq 0.05$ *vs* D0 at D1,2&3 post LPS in all LPS treated groups, Fig. 1H). A positive effect of Tβ4 emerged in APP/PS1, but not WT, mice from the 3rd day of treatment until the end of the experiment, with an improved burrowing performance regardless of LPS (PBS *vs* Tβ4: $p = 0.04$, Fig. 1G; LPS *vs* LPS+ Tβ4: $p = 0.002$, Fig. 1 H).

3.1.3. LPS-induced locomotor suppression

Acute sickness was monitored through the distance moved in the open field for 3 min prior to and at 2, 4 and 6 h post LPS administration, while recovery was tracked at 24 h, 3 and 7 days post-LPS. Baseline ambulatory activity did not differ between the genotypes ($t_{(57)} = 0.69$, $p = 0.49$, Fig. 2A). Whilst the distance moved in the open-field arena was reduced by repeated testing, locomotor suppression was overall more pronounced in LPS-treated mice (LPS X Time: $F_{(1,6)} = 9.13$, $p < 0.0001$; Fig. 2B), for up to 24 h after inoculation, regardless of the genotype and treatment withTβ4 ($p < 0.05$ at 2, 4, 6 and 24 h post-LPS in both WT and APP/PS1 mice).

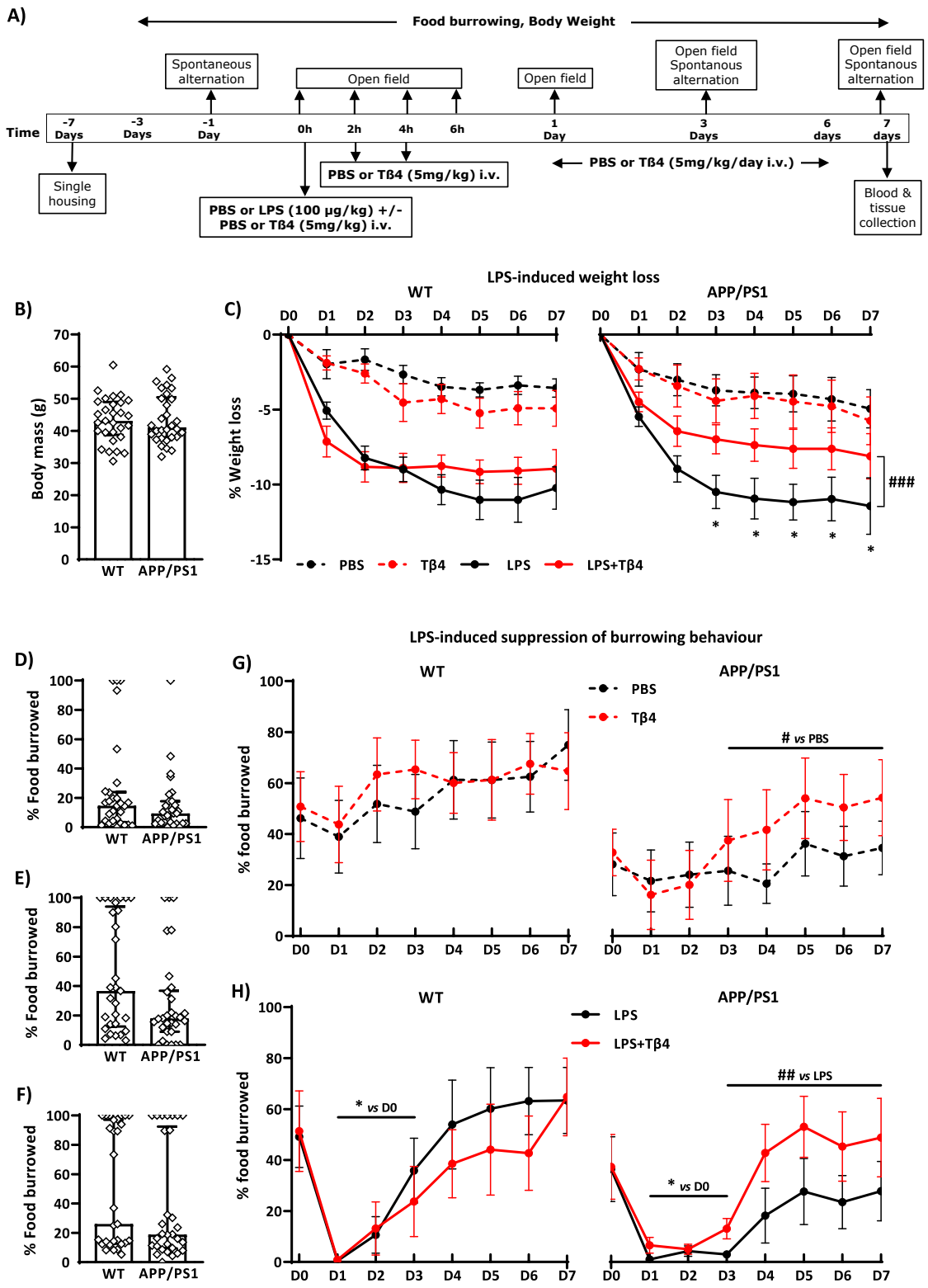

Fig. 1. A) Timeline of the experiment. B) Body mass recorded prior to PBS and/or LPS and/or Tß4 administration did not differ between genotypes. C) Body weight decreased over the 7 days, to a greater extent in mice inoculated with LPS (100 µg/kg i.v.), regardless of Tß4 treatment. Tß4 (5 mg/kg *i.v.* at 0, 2 and 4 h post-LPS and then once daily for another 6 days) alleviated LPS-induced weight loss in APP/PS1 mice but reduced the body weight of WT mice in the absence of LPS. D-E-F) Baseline food burrowing performance on days −3, −2, −1 prior to the LPS challenge did not differ significantly between the genotypes. F-G). Over the 7 days of treatment, food burrowing behaviour was lower in APP/PS1 mice than in their WT littermates ($F_{(1,51)} = 6.98$, $p = 0.01$). LPS significantly suppressed food burrowing behaviour regardless of the genotype and treatment with Tß4 for 3 days post LPS ($p \leq 0.05$ *vs* D0 at D1,2&3 post-LPS for all four LPS-treated groups). Tβ4 improved the food burrowing performance of APP/PS1, but not WT mice from the third day of treatment, regardless of LPS. B,D,E,F) Data are expressed as Median ± interquartile range. Squares represent individual animals. C,G,H) Data expressed as Means ± SEM. Pairwise comparisons: *$p < 0.05$ vs LPS + Tβ4 (C) or D0 (C,H). # $p < 0.05$, ## $p < 0.01$, ### $p < 0.0001$. n = 7–6 per group.

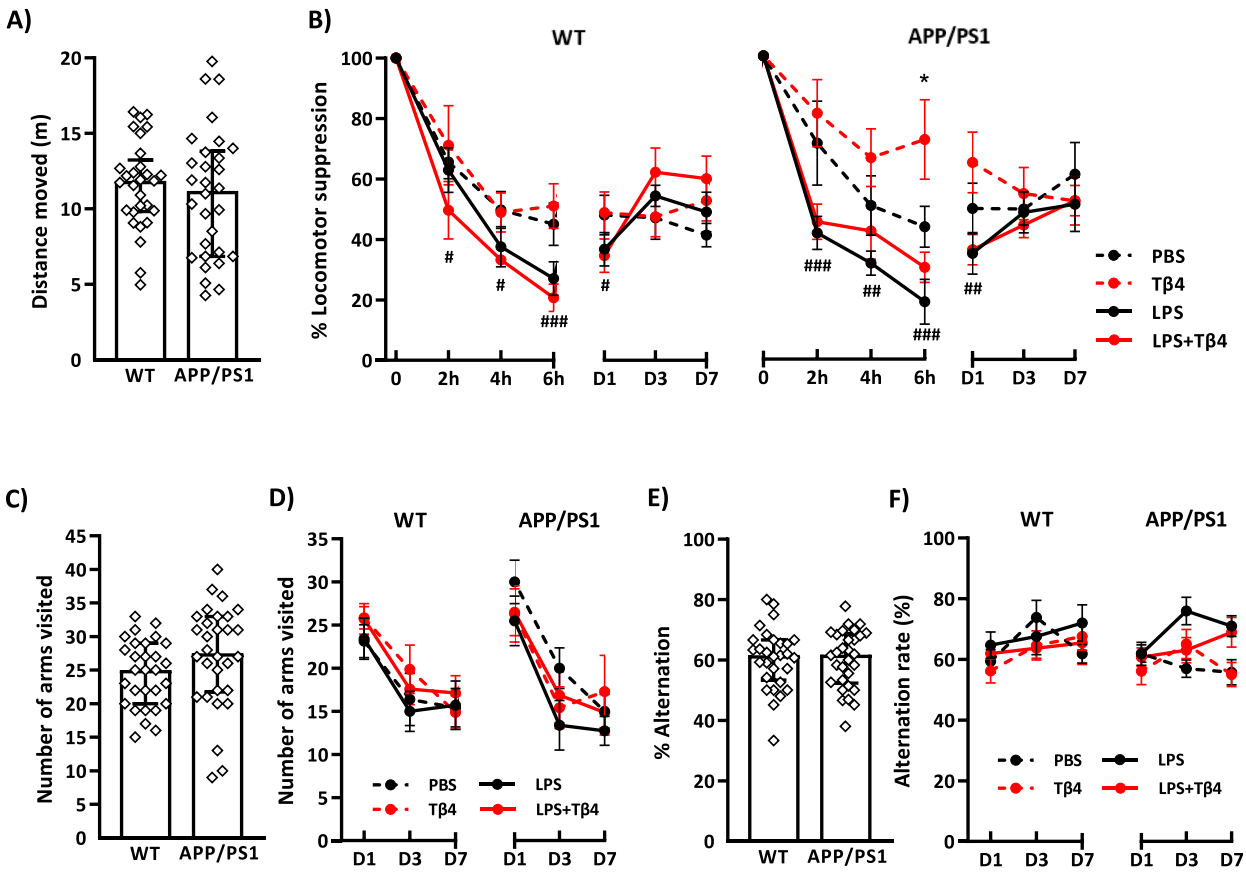

Fig. 2. Ambulatory activity in the open-field was repeatedly assessed prior to and after onset of treatments to monitor the acute LPS-induced sickness at 2, 4, and 6 h post-LPS, and its recovery at 1, 3 and 7 days post-LPS. A) Baseline locomotor performance on D0 prior to the injections did not differ significantly between the genotypes. B) Locomotor performance, expressed as percentage of baseline values, decreased with repeated testing, but to a greater extent in LPS-treated mice (LPS X Time: $F_{(1,6)} = 9.13$, $p < 0.0001$), for up to the 24 h time point, in both genotypes. C,E) APP/PS1 and WT mice also did not differ for the exploratory drive (C) and spatial working memory performance (E) in the spontaneous alternation test prior to any treatment. D) The number of arm visits significantly decreased with repeated testing in all groups ($F_{(2,101)} = 94.73$, $p < 0.0001$), particularly between D0 and D3 ($p \leq 0.01$ in all groups). It plateaued in all treatment groups but Tβ4-treated WT mice and PBS-treated APP/PS1 mice between the 3rd and 7th day post LPS ($p = 0.04$ in both cases). F) The number of arms visited was a significant covariate for spatial working memory performance ($F_{(2,100)} = 14.7$, $p = 0.0002$). While there was an overall significant effect of LPS on spatial working memory performance ($F_{(2,51)} = 6.00$, $p = 0.017$), the alternation rate did not differ significantly between the experimental groups. A, C,E) Data are expressed as Median ± interquartile range. Squares represent individual animals. B, D, F) Data expressed as Means ± SEM. Pairwise comparisons: *$p < 0.05$ *vs* PBS-treated APP/PS1 mice. LPS *vs* non-LPS treated mice: # $p < 0.05$, ## $p < 0.01$, ### $p < 0.0001$. N = 7–8 per group.

3.1.4. Spontaneous alternation behaviour was unaffected by LPS and/or Tβ4

Baseline exploratory drive and spatial working memory performance prior to the injections did not differ between APP/PS1 and WT mice ($t_{(57)} = -1.49$, $p = 0.14$ and $t_{(57)} = 0.12$, $p = 0.90$, Fig. 2C&E, respectively). The number of arms visits decreased significantly with repeated testing regardless of LPS and/or Tβ4 ($F_{(2,101)} = 94.73$, $p < 0.0001$), with a sharp decrease between baseline measurements and the 3rd day post -LPS ($p \leq 0.01$ in all groups). It then plateaued in all groups but Tβ4-treated WT mice and PBS-treated APP/PS1 mice (D3 *vs* D7: $p = 0.04$ in both cases, Fig. 2D). While there was an overall significant effect of LPS on spatial working memory performance ($F_{(2,51)} = 6.00$, $p = 0.017$), pairwise comparisons did not reveal any significant fluctuations in the alternation rate between any of the experimental groups (Fig. 2F).

3.2. Tβ4 alleviates LPS-induced plaque load in the hippocampus and cortex of APP/PS1 mice

In the hippocampus, Tβ4 effectively prevented the increase in amyloid plaque load induced by LPS, assessed through the number of plaques per mm^2 (LPS × Tβ4: $F_{(1,25)} = 5.27$, $p = 0.03$; Fig. 3A&B) and the percentage area stained (LPS × Tβ4: $F_{(1,25)} = 13.31$, $p = 0.0012$; Fig. 3C). The effects of LPS and co-treatment with Tβ4 were particularly seen on the number of small and large plaques (LPS × Tβ4: $F_{(1,25)} = 4.26$, $p = 0.049$ and $F_{(1,25)} = 12.38$, $p = 0.002$, respectively, Fig. 3B). For all these measures, LPS-treated mice showed greater amyloid plaque load than both PBS- and LPS+Tβ4-treated mice ($p \leq 0.01$ in all cases, Fig. 3B, C,D&E). In the cortex, a significant prevention by Tβ4 was only seen on the number of large plaques (LPS × Tβ4: $F_{(1,26)} = 7.55$, $p = 0.01$; Fig. 4B), increased area covered by Aß (LPS × Tβ4: $F_{(1,26)} = 5.88$, $p = 0.02$, Fig. 4C) and APP concentrations (LPS × Tβ4: $F_{(1,26)} = 4.4$, $p = 0.045$, Fig. 4D), whereas levels of soluble Aß1-40 were unaltered (Fig. 4E). While LPS had no impact on the average plaque size, the area of small hippocampal plaques was significantly increased in Tβ4-treated mice, regardless of LPS ($F_{(1,25)} = 7.52$, $p = 0.01$; Fig. 3D). In the cortex, the area of both medium and large plaques was reduced by Tβ4 in PBS-treated ($F_{(1,26)} = 5.32$, $p = 0.03$) and LPS-treated ($F_{(1,26)} = 5.06$, $p = 0.03$) mice, respectively (Fig. 4F).

3.3. Tβ4 increases astrocyte and microglial proliferation in the hippocampus of LPS-treated WT mice

APP/PS1 mice showed a higher density of both astrocyte ($F_{(1,51)} = 25.15$, $p < 0.0001$; Fig. 5B) and microglia ($F_{(1,50)} = 4.95$, $p = 0.03$;

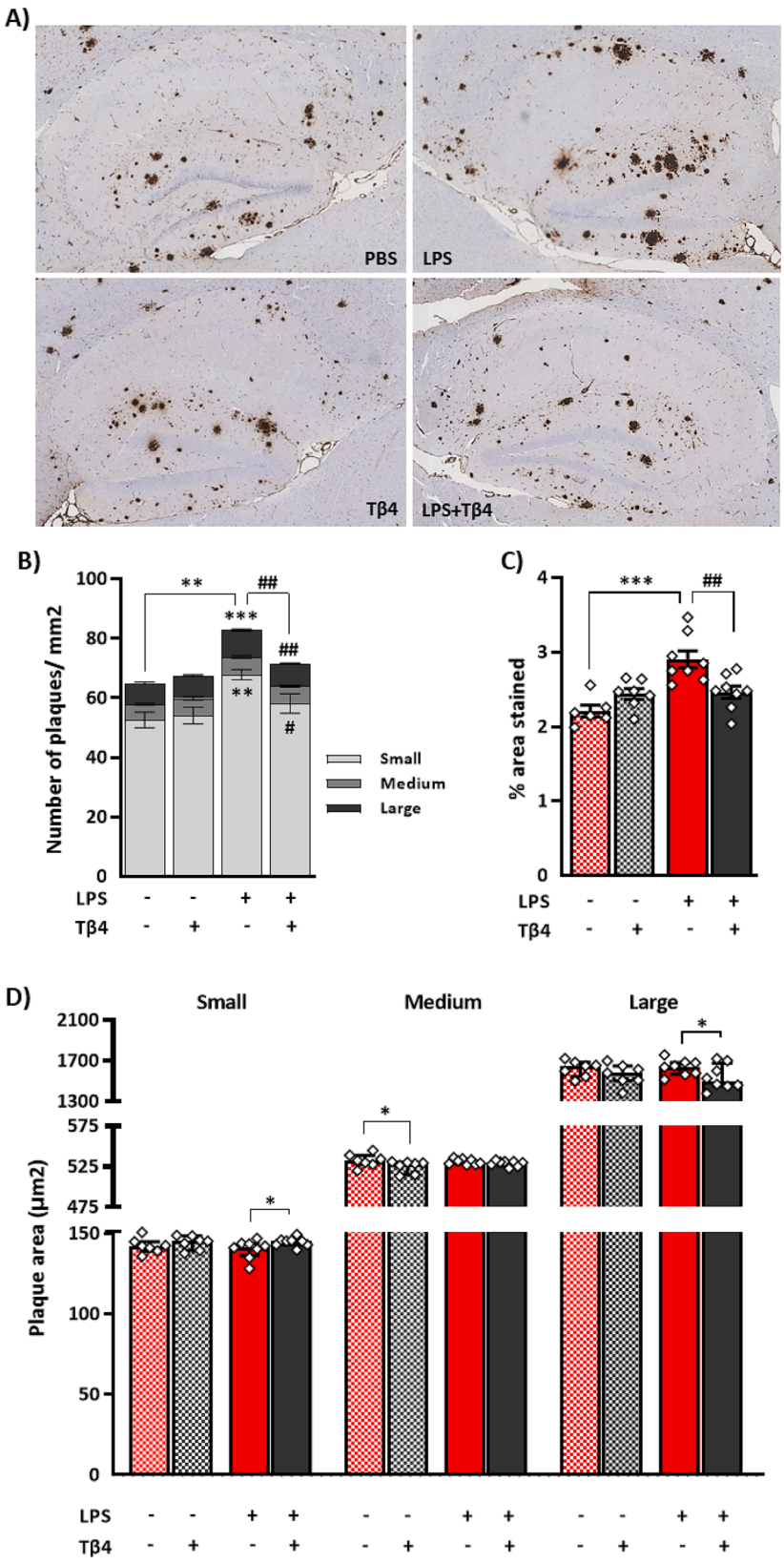

Fig. 3. A) Representative images of Aß immunostaining in the whole hippocampus of 12.5-month-old APP/PS1 challenged with LPS (100 µg/kg i.v) or PBS and treated with PBS or Tß4 (5 mg/kg *i.v.*) at 0, 2 and 4 h post-LPS and then once daily for another 6 days. B, C) Hippocampal amyloid plaque load was significantly increased by LPS, and this was alleviated by co-treatment with Tß4. The increased plaque number (B) and percentage area covered by Aß (C) seen in LPS-treated mice, but prevented by Tß4, was due to preferential increases in the number of small and large plaques (C). The average areas of small (≤400 µm^2), medium (401 µm^2–700 µm^2) and large (>700 µm^2) plaques, was unaffected by LPS. The area of small plaques was overall larger in Tβ4-treated mice regardless of LPS ($F_{(1,25)} = 7.52$, $p = 0.01$), but none of the partial comparisons was significant. Data expressed as median ± interquartile range. Squares represent individual animals. Pairwise comparisons: **p < 0.01, ***p < 0.0001 vs PBS. # p < 0.05, ## p < 0.01, vs LPS. n = 6–8 per group.

Fig. 5D) as well as larger microglial somas ($F_{(1,50)} = 5.72$, $p = 0.0002$; Fig. 5E) than WT mice, while controlling for the number of microglial clusters ($F_{(1,50)} = 31.17$, $p < 0.0001$ and $F_{(1,50)} = 66.39$, $p < 0.0001$, respectively) made of enlarged microglia that typically surround the plaques (Fig. 5C). Effects of LPS were only seen in WT mice, with an increased in microglia soma areas regardless of Tβ4 (Genotype × LPS: $F_{(1,50)} = 7.57$, $p = 0.0008$; Fig. 5E) whereas co-treatment of LPS with Tβ4 resulted in an increased astrocytic ($p < 0.05$ *vs* both PBS and LPS-treated WT mice, Fig. 5B) and microglial density ($p < 0.01$ *vs* both PBS and LPS-treated WT mice, Fig. 5D).

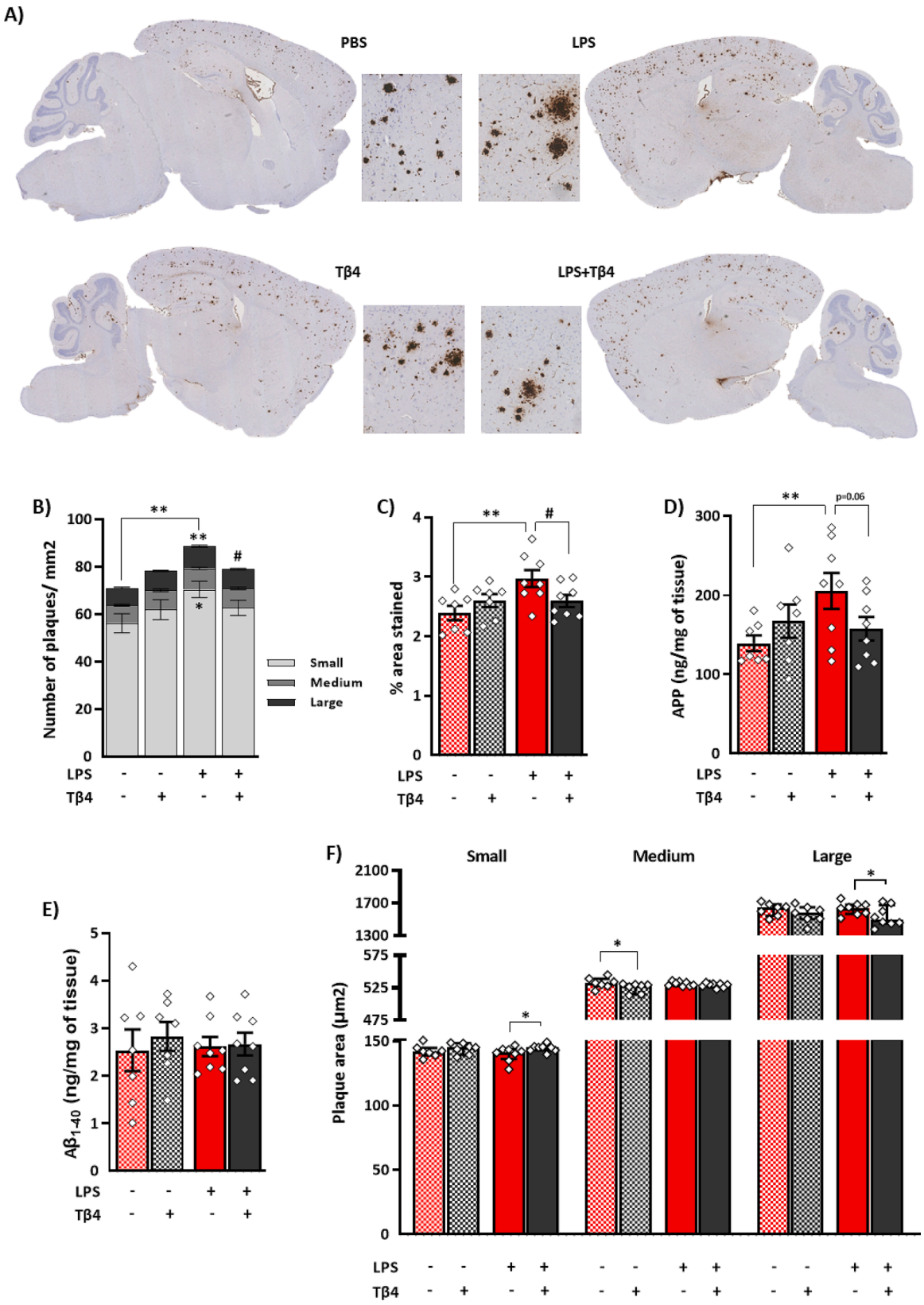

Fig. 4. A) Representative images of Aß immunostaining in the whole brain and cortex of 12.5-month-old APP/PS1 mice challenged with LPS (100 µg/kg i.v) or PBS and treated with PBS or Tß4 (5 mg/kg *i.v.*) at 0, 2 and 4 h post-LPS and then once daily for another 6 days. B, C) Cortical amyloid plaque load was significantly increased by LPS, and this was alleviated by co-treatment with Tß4. The increased plaque number seen in LPS-treated mice but the significant prevention by Tß4 was only seen on the number of large plaques (B). Tß4 also prevented the LPs-induced increased in the percentage area covered by Aß (C) and APP concentrations (D), but the levels of soluble Aß1-40 were unaltered (E). The average areas of small ($\leq$400 µm^2), medium (401 µm^2–700 µm^2) and large (>700 µm^2) plaques, were unaffected by LPS. The area of medium plaques was reduced by Tβ4 in PBS-treated mice, but the area of large plaques was reduced by Tβ4 in LPS-treated mice. Data expressed as

median ± interquartile range. Squares represent individual animals. Pairwise comparisons: *p < 0.05, **p < 0.01 vs PBS. # p < 0.05, ## p < 0.01, vs LPS. n = 6–8 per group.

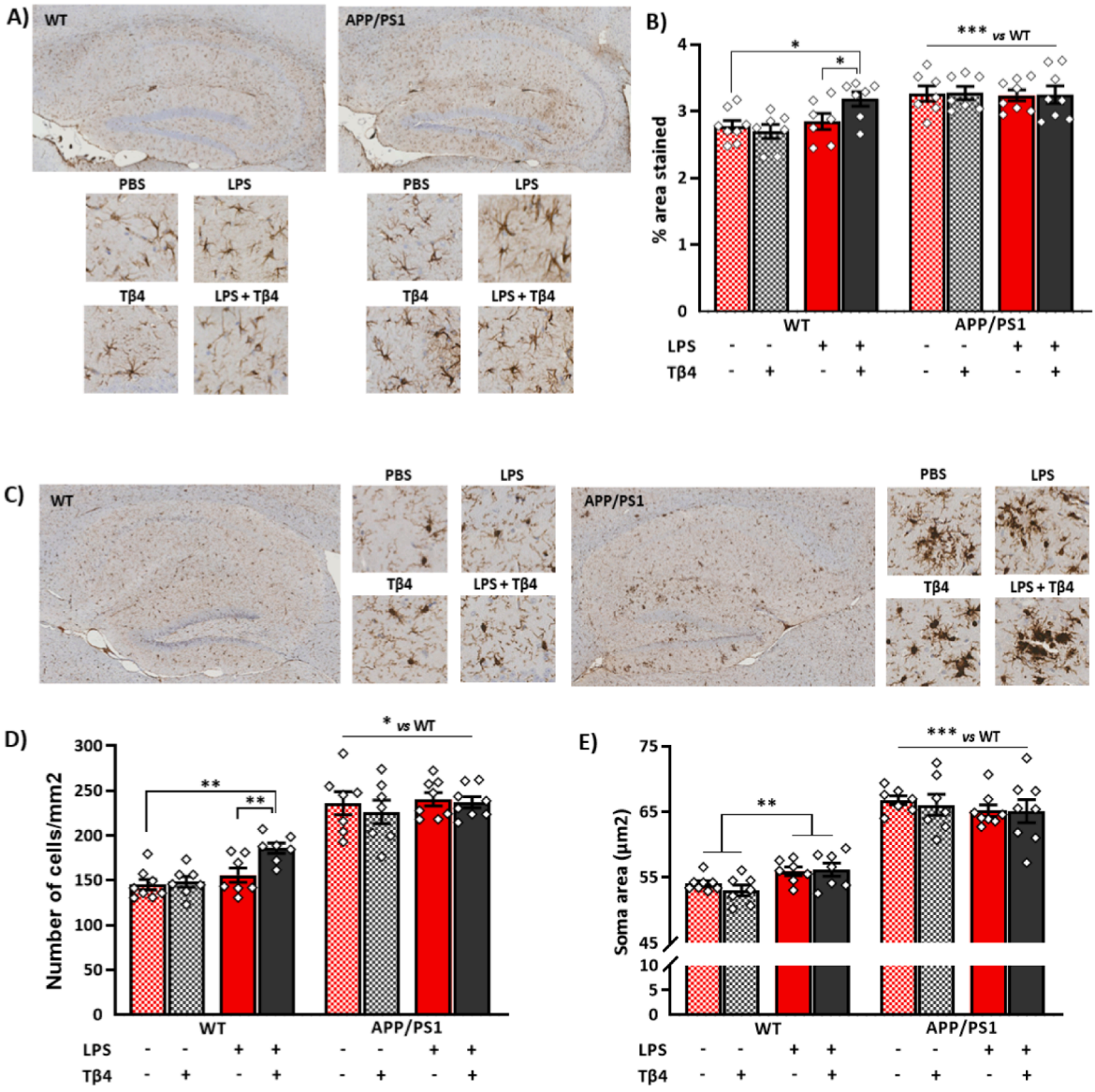

Fig. 5. A) Representative images of GFAP immunostaining in the whole hippocampus of 12.5-month-old APP/PS1 mice challenged with LPS (100 µg/kg i.v) or PBS and treated with PBS or Tß4 (5 mg/kg *i.v.*) at 0, 2 and 4 h post-LPS and then once daily for another 6 days. B) APP/PS1 mice exhibited higher astrocytic density, but the significant genotype X LPS interaction ($F_{(1,51)} = 4.39$, $p = 0.04$) was caused by a selective increase in the percentage area stained by GFAP in WT mice co-treated with LPS and Tß4. C) Representative images of Iba1 immunostaining in the whole hippocampus of 12.5-month-old APP/PS1 challenged with LPS or PBS and then treated with PBS or Tß4. Microgliosis occurred in APP/PS1 mice, as reflected by the higher number of microglial cells (D) and soma area (E) indicative of an activated phenotype. Co-treatment of LPS-treated WT mice with Tß4 increased microglial proliferation (D), but microglial somas were enlarged in the hippocampus of WT mice 7 days after the LPS challenge, regardless of Tß4 (E). (B). Data expressed as median ± interquartile range. Squares represent individual animals. Pairwise comparisons: **p < 0.01, ***p < 0.0001 vs PBS. n = 7–8 per group.

4. Discussion

LPS is thought to play a critical role in AD pathogenesis [5,6,8,9]. Consistent with this hypothesis, we found that an acute low LPS dose was sufficient to exacerbate amyloid plaque load in 12.5-month-old APP/PS1 mice. Since Tß4 was found effective to limit the impact of septic LPS doses on lethality and circulating pro-inflammatory cytokine levels when administered from immediately after LPS [13], we hypothesised that such treatment regimen would counteract the effect of low-dose LPS on pathological features of AD. Our main findings show that Tß4 effectively blocked LPS-induced plaque load, while also reducing the severity of LPS-induced sickness. The benefits of Tß4 on sickness symptoms were more noticeable in APP/PS1 mice than in their WT littermates despite their higher sickness response. Yet, in WT mice, Tß4 selectively induced astrocyte and microglial proliferation in the hippocampus.

Both the dose and the timing of administration were reported to be critical factors in determining the impact of Tß4 on survival after a lethal

LPS dose in mice, with a 100% survival rate when Tß4 was first administered at a dose of 5 mg/kg immediately after LPS and then 2 and 4 h later [13]. We applied this most effective Tß4 treatment regimen, but despite continuing the treatment for 7 days, and using a low LPS dose (100 ug/kg *vs* 60 mg/kg in [13]), this was not sufficient to fully prevent LPS-induced sickness. One possible explanation is the age of the mice used in this study, corresponding to middle age, as susceptibility to LPS is well known to increase with aging, whereby sublethal LPS doses for young mice were associated with prolonged behavioural sickness [21] as well as increased mortality and circulating pro-inflammatory cytokines levels from middle age [27], but the greater efficacy of Tß4 in APP/PS1 mice, which are also the most susceptible to LPS, argues against, this hypothesis. LPS-induced sickness which is observed even at extremely low doses (e.g. 1 ug/kg) below the threshold to induce overt inflammation, was found independent of cytokines levels [28]. Prostaglandin E2 (PGE2) is thought to be the major driver of LPS-induced sickness [29], and while Tß4 effectively reduced PGE2 production induced by LPS or pro-oxidants *in vitro*, this was found to be dose-dependent [30,31], suggesting that higher Tß4 doses may be more effective against the sickness syndrome.

In contrast, our chosen Tß4 treatment regimen was highly effective in preventing LPS-induced Aß plaque load, particularly in the hippocampus. A single LPS challenge resulted in an increased number of small and large plaques, suggesting that it promoted both Aß production and plaque maturation. This is agreement with reports from several groups showing that LPS can stimulate both Aß generation and aggregation (for review [9]). Aß is generated from APP [32] and our cortical data showing that changes in APP concentrations mirror those of small plaques number, indicate that Tß4 has the potential to block the LPS-induced Aß production. An effect on LPS-induced plaque maturation and growth cannot be fully established from our data since the restricting effects of Tß4 on plaque size were rather subtle and not specific to LPS-treated mice. There is strong evidence to suggest that the pro-inflammatory cytokine tumor necrosis factor alpha (TNF-α) is a critical mediator of systemic inflammation-induced Aß load, through its ability to enter the brain and promote abnormal amyloid metabolism [33]. Tß4 was found to lower LPS-induced TNF-α production [13] and to be an effective inhibitor of TNF-α signalling [34], suggesting that it may, at least in part, prevent LPS-induced plaque load by modulating TNF-α-mediated inflammation.

Reactive gliosis associates with plaques, but activated astrocytes and microglia become dysfunctional as AD progresses, which compromises their ability to inhibit plaque formation and growth [35,36]. Due to their advanced pathological stage, the hippocampi of APP/PS1 mice exhibited a higher density of astrocytes and microglial presenting with the morphological features of a pro-inflammatory detrimental phenotype that would favour Aß deposition. Overexpression of Tß4 in the hippocampus was recently reported to significantly reduce the progression of Aß burden while also preserving the healthier phenotype of glial cells and downregulating pro-inflammatory signalling in the brain [37]. Here we did not observe any effect of LPS or Tß4 treatment on gliosis in APP/PS1. While this may be related to the advanced pathological stage of the mice and /or the 7-day delay after inoculation with LPS, Tß4 may not have entered the brain in sufficient amount to affect glial cells activation as its recovery in the brain was found not to exceed 4% at 20 mins to 2 h post-systemic injection [38].

Consistent with our earlier findings [18], we found here that microglial somas were enlarged in the hippocampus of LPS-treated WT but not APP/PS1 mice, indicating microglial activation, but this was independent of Tß4 treatment. In WT mice, however, Tß4 treatment following inoculation with LPS led to an increased density of microglia and astrocytes, suggesting an enhancement of glial proliferation. The functional significance of this increased gliosis remains to be determined as it occurred without presenting the morphological features of a detrimental phenotype. And, in particular, enlargement of microglial somas by LPS, an indicator of microglial activation, occurred to the same extent with or without co-treatment Tß4. Under normal conditions, reactive gliosis is a protective response to the brain, designed to combat tissue damage and to promote neural remodelling [39] and Tß4 has well established neuroprotective and neurorestorative functions [40].

Excess levels of LPS are thought to play a pivotal role in mediating the exacerbating effect of systemic infection and inflammation on AD progression [27]. Altogether, our data highlight the potential of Tß4 in controlling the deleterious effect of LPS on AD progression during systemic inflammation.

CRediT authorship contribution statement

Othman Othman: Investigation. **Hayley Marshall:** Investigation. **Mitchell Masterson:** Investigation. **Poppy Winlow:** Investigation. **Graham Gibson:** Methodology. **Yuchun Ding:** Methodology, Software. **Marie-Christine Pardon:** Conceptualization, Project administration, Formal analysis, Supervision, Funding acquisition.

Declaration of Competing Interest

The authors declare that they have no known competing financial interests or personal relationships that could have appeared to influence the work reported in this paper.

Data availability

Data will be made available on request.

Acknowledgments

This work was supported by Medical Research Council Proximity to Discovery Awards [Grant Number MC_PC_14121 & MC_PC_17173] to MCP. We thank RengeneRx Biopharmaceuticals for the generous gift of Thymosin beta 4.

References:

[1] P. Maheshwari, G.D. Eslick, Bacterial infection and Alzheimer's disease: a meta-analysis, J. Alzheimers Dis. 43 (3) (2015) 957–966.
[2] D. Liccardo, et al., Potential Bidirectional Relationship Between Periodontitis and Alzheimer's Disease, Front. Physiol. 11 (2020) 683.
[3] B. Giunta, et al., Inflammaging as a prodrome to Alzheimer's disease, J. Neuroinflammation 5 (2008) 51.
[4] M.A. Batista, et al., Inflammaging in Endemic Areas for Infectious Diseases, Front. Immunol. 11 (2020), 579972.
[5] G.C. Brown, The endotoxin hypothesis of neurodegeneration, J. Neuroinflammation 16 (1) (2019) 180.
[6] X. Zhan, B. Stamova, F.R. Sharp, Lipopolysaccharide Associates with Amyloid Plaques, Neurons and Oligodendrocytes in Alzheimer's Disease Brain: A Review, Front. Aging Neurosci. 10 (2018) 42.
[7] R. Zhang, et al., Circulating endotoxin and systemic immune activation in sporadic amyotrophic lateral sclerosis (sALS), J. Neuroimmunol. 206 (1–2) (2009) 121–124.
[8] M. Sochocka, et al., The Gut Microbiome Alterations and Inflammation-Driven Pathogenesis of Alzheimer's Disease-a Critical Review, Mol. Neurobiol. 56 (3) (2019) 1841–1851.
[9] H.S. Kim, et al., Gram-negative bacteria and their lipopolysaccharides in Alzheimer's disease: pathologic roles and therapeutic implications, Transl Neurodegener 10 (1) (2021) 49.
[10] S.M. Opal, Endotoxins and other sepsis triggers, Contrib. Nephrol. 167 (2010) 14–24.
[11] E. Hannappel, et al., Thymosin beta 4: a ubiquitous peptide in rat and mouse tissues, PNAS 79 (7) (1982) 2172–2175.
[12] J. Zhang, et al., Association between Thymosin beta-4, acute kidney injury, and mortality in patients with sepsis: An observational cohort study, Int. Immunopharmacol. 101 (Pt A) (2021), 108167.
[13] M. Badamchian, et al., Thymosin beta(4) reduces lethality and down-regulates inflammatory mediators in endotoxin-induced septic shock, Int. Immunopharmacol. 3 (8) (2003) 1225–1233.
[14] A. Agostini, et al., Sex-specific hippocampal metabolic signatures at the onset of systemic inflammation with lipopolysaccharide in the APPswe/PS1dE9 mouse model of Alzheimer's disease, Brain Behav. Immun. 83 (2020) 87–111.
[15] M.R. Barron, et al., Increasing Tau 4R Tau Levels Exacerbates Hippocampal Tau Hyperphosphorylation in the hTau Model of Tauopathy but Also Tau Dephosphorylation Following Acute Systemic Inflammation, Front. Immunol. 11 (2020) 293.

[16] C. Kilkenny, et al., Improving bioscience research reporting: the ARRIVE guidelines for reporting animal research, PLoS Biol. 8 (6) (2010) e1000412.
[17] J.L. Jankowsky, et al., Mutant presenilins specifically elevate the levels of the 42 residue beta-amyloid peptide in vivo: evidence for augmentation of a 42-specific gamma secretase, Hum. Mol. Genet. 13 (2) (2004) 159–170.
[18] M.C. Pardon, et al., Magnetic Resonance Spectroscopy discriminates the response to microglial stimulation of wild type and Alzheimer's disease models, Sci. Rep. 6 (2016) 19880.
[19] R. Zhao, et al., Microglia limit the expansion of beta-amyloid plaques in a mouse model of Alzheimer's disease, Mol. Neurodegener. 12 (1) (2017) 47.
[20] M. Meyer-Luehmann, et al., Rapid appearance and local toxicity of amyloid-beta plaques in a mouse model of Alzheimer's disease, Nature 451 (7179) (2008) 720–724.
[21] J.P. Godbout, et al., Aging exacerbates depressive-like behavior in mice in response to activation of the peripheral innate immune system, Neuropsychopharmacology 33 (10) (2008) 2341–2351.
[22] R.M. Deacon, A. Croucher, J.N. Rawlins, Hippocampal cytotoxic lesion effects on species-typical behaviours in mice, Behav. Brain Res. 132 (2) (2002) 203–213.
[23] Y. Ding, et al., Novel Methods for Microglia Segmentation, Feature Extraction, and Classification, IEEE/ACM Trans. Comput. Biol. Bioinf. 14 (6) (2017) 1366–1377.
[24] K. Scheffler, et al., Determination of spatial and temporal distribution of microglia by 230nm-high-resolution, high-throughput automated analysis reveals different amyloid plaque populations in an APP/PS1 mouse model of Alzheimer's disease, Curr. Alzheimer Res. 8 (7) (2011) 781–788.
[25] B.T. Casali, G.E. Landreth, Abeta Extraction from Murine Brain Homogenates, Bio Protoc 6 (8) (2016).
[26] S.T. Bate, R.A. Clark, S.C. Stanford, Using InVivoStat to perform the statistical analysis of experiments, J. Psychopharmacol. 31 (6) (2017) 644–652.
[27] P.R. Mouton, et al., The effects of age and lipopolysaccharide (LPS)-mediated peripheral inflammation on numbers of central catecholaminergic neurons, Neurobiol Aging 33(2) (2012) 423 e27-36.
[28] J.L. Teeling, et al., Sub-pyrogenic systemic inflammation impacts on brain and behavior, independent of cytokines, Brain Behav. Immun. 21 (6) (2007) 836–850.
[29] C.B. Saper, A.A. Romanovsky, T.E. Scammell, Neural circuitry engaged by prostaglandins during the sickness syndrome, Nat. Neurosci. 15 (8) (2012) 1088–1095.
[30] D. Hwang, et al., Anti-Inflammatory Activity of beta-thymosin Peptide Derived from Pacific Oyster (Crassostrea gigas) on NO and PGE(2) Production by Down-Regulating NF-kappaB in LPS-Induced RAW264.7 Macrophage Cells, Mar. Drugs 17 (2) (2019).
[31] S.I. Lee, et al., Thymosin Beta-4 Suppresses Osteoclastic Differentiation and Inflammatory Responses in Human Periodontal Ligament Cells, PLoS One 11 (1) (2016) e0146708.
[32] Y.W. Zhang, et al., APP processing in Alzheimer's disease, Mol. Brain 4 (2011) 3.
[33] B. Decourt, D.K. Lahiri, M.N. Sabbagh, Targeting Tumor Necrosis Factor Alpha for Alzheimer's Disease, Curr. Alzheimer Res. 14 (4) (2017) 412–425.
[34] P. Qiu, et al., Thymosin beta4 inhibits TNF-alpha-induced NF-kappaB activation, IL-8 expression, and the sensitizing effects by its partners PINCH-1 and ILK, FASEB J. 25 (6) (2011) 1815–1826.
[35] G.R. Frost, Y.M. Li, The role of astrocytes in amyloid production and Alzheimer's disease, Open Biol. 7 (12) (2017).
[36] D.V. Hansen, J.E. Hanson, M. Sheng, Microglia in Alzheimer's disease, J. Cell Biol. 217 (2) (2018) 459–472.
[37] M. Wang, et al., Thymosin beta4 reverses phenotypic polarization of glial cells and cognitive impairment via negative regulation of NF-kappaB signaling axis in APP/PS1 mice, J. Neuroinflammation 18 (1) (2021) 146.
[38] C.A. Mora, et al., Biodistribution of synthetic thymosin beta 4 in the serum, urine, and major organs of mice, Int. J. Immunopharmacol 19 (1) (1997) 1–8.
[39] J.E. Burda, M.V. Sofroniew, Reactive gliosis and the multicellular response to CNS damage and disease, Neuron 81 (2) (2014) 229–248.
[40] M. Chopp, Z.G. Zhang, Thymosin beta4 as a restorative/regenerative therapy for neurological injury and neurodegenerative diseases, Expert Opin. Biol. Ther. 15 (Suppl. 1) (2015) S9–S.